AMERICAN SOCIETY FOR MICROBIOLOGY | Molecular and Cellular Biology®

RESEARCH ARTICLE

E2F6-Mediated Downregulation of MIR22HG Facilitates the Progression of Laryngocarcinoma by Targeting the miR-5000-3p/FBXW7 Axis

Hui Chen,[a] Mudunov Ali,[b] Azizyan Ruben,[b] Dimitry Stelmakh,[b] Maksim Pak[b]

[a]I. M. Sechenov First Moscow State Medical University, Moscow, Russian Federation
[b]N. N. Blokhin National Medical Research Center of the Oncology of the Ministry of Health of the Russian Federation, Moscow, Russian Federation

ABSTRACT Recently, abundant evidence has clarified that long noncoding RNAs (lncRNAs) play an oncogenic or anticancer role in the tumorigenesis and development of diverse human cancers. Described as a crucial regulator in some cancers, MIR22HG has not yet been studied in laryngocarcinoma and therefore the underlying regulatory role of MIR22HG in laryngocarcinoma is worth detecting. In this study, MIR22HG expression in laryngocarcinoma cells was confirmed to be downregulated, and upregulated MIR22HG expression led to suppressive effects on laryngocarcinoma cell proliferation and migration. Molecular mechanism assays revealed that MIR22HG sponges miR-5000-3p in laryngocarcinoma cells. Besides, decreased expression of miR-5000-3p suppressed laryngocarcinoma cell proliferation and migration. Moreover, the FBXW7 gene was reported to be a downstream target gene of miR-5000-3p in laryngocarcinoma cells. More importantly, rescue assays verified that FBXW7 depletion or miR-5000-3p upregulation countervailed the repressive effects of MIR22HG overexpression on laryngocarcinoma progression. In addition, E2F6 was proved to be capable of inhibiting MIR22HG transcription in laryngocarcinoma cells. To sum up, E2F6-induced downregulation of MIR22HG promotes laryngocarcinoma progression through the miR-5000-3p/FBXW7 axis.

KEYWORDS MIR22HG, miR-5000-3p, FBXW7, E2F6, laryngocarcinoma

Diagnosed as the most prevalent malignancy with high incidence and mortality, laryngocarcinoma belongs to head and neck cancer types accounting for about 25 to 30% of cancer-related cases worldwide (1, 2). In recent years, the death rate from laryngocarcinoma in countries with developed health care systems has decreased. Nevertheless, laryngocarcinoma-related complications, including cough, trachyphonia, and dysphagia, as well as dyspnea, gave rise to much pain to in patients (3, 4). Reports have revealed that laryngocarcinoma patients at an early stage have a cure rate of about 85%, while patients with the advanced stage have just a 60% chance of cure (5). Surgical resection is thought to be an effective treatment for laryngocarcinoma patients at an early stage (6). Nonetheless, because of the lack of an early and effective diagnosis biomarker, the majority of the laryngocarcinoma patients were diagnosed with advanced-stage metastasis, leading to a disappointing survival rate (7–10). Thus, exploring crucial molecules and biomarkers underlying laryngocarcinoma progression is of great importance for finding efficient strategies for laryngocarcinoma treatment.

Abundant evidence has suggested that only 1.2% of the genome is capable of encoding proteins in mammals (11, 12). The major part of genome is transcribed into long noncoding RNAs (lncRNAs), a main subtype of noncoding RNAs (ncRNAs) with a lengths exceeding 200 nucleotides (13, 14). In addition, lncRNAs have been considered RNA molecules with no or limited capacity of protein coding owing to the lack of an

Citation Chen H, Ali M, Ruben A, Stelmakh D, Pak M. 2020. E2F6-mediated downregulation of MIR22HG facilitates the progression of laryngocarcinoma by targeting the miR-5000-3p/FBXW7 axis. Mol Cell Biol 40:e00496-19. https://doi.org/10.1128/MCB.00496-19.

Address correspondence to Mudunov Ali, ali.mudunov@inbox.ru.

Received 10 October 2019
Returned for modification 19 October 2019
Accepted 20 February 2020
Accepted manuscript posted online 24 February 2020
Published 28 April 2020

open reading structure of a required length (15, 16). Previous studies have emphasized the relation between lncRNAs and molecular mechanisms in tumor progression and also verified the value of lncRNAs as promising biomarkers (17). A growing number of investigations have clarified that lncRNAs exerted vital effects on the regulation of tumor behaviors (18, 19). Moreover, dysregulation of lncRNAs has been found to regulate the progression of various cancers via the competing endogenous RNA (ceRNA) network. For example, lncRNA LOXL1-AS1 contributes to prostate cancer progression by sponging miR-541-3p and targeting CCND1 (20). lncRNA EPB41L4A-AS2 inhibits hepatocellular carcinoma via the miR-301a-5p/FOXL1 axis (21). Although the MIR22 host gene (MIR22HG) has been researched and identified as an oncogene in several cancers (22, 23), its regulatory role in laryngocarcinoma remains to be explored.

In the present study, we attempted to decipher the regulatory mechanism of MIR22HG in laryngocarcinoma. The results of multiple assays applied in this study reveal that E2F6-mediated MIR22HG downregulation promotes laryngocarcinoma progression via the miR-5000-3p/FBXW7 axis, suggesting a new therapeutic target for laryngocarcinoma.

RESULTS

MIR22HG is expressed at low levels, and its upregulation inhibits cell proliferation and migration in laryngocarcinoma. Although low expression of MIR22HG has been detected in several cancers (22, 23), its expression status in laryngocarcinoma cells remains to be analyzed. As illustrated in Fig. 1A, MIR22HG expression was dramatically lower in laryngocarcinoma cell lines (UM-SCC-10B, SNU899 and SNU46) than in a normal nasopharyngeal epithelial cell line (NP69). In order to detect the biological function of MIR22HG in laryngocarcinoma, we first overexpressed MIR22HG in SNU46 and SNU899 cells utilizing pcDNA3.1/MIR22HG (Fig. 1B). Afterward, cell proliferation assays, including CCK-8, colony formation, and 5-ethynyl-2′-deoxyuridine (EdU) assays, showed that overexpression of MIR22HG had a suppressive impact on cell proliferation (Fig. 1C to E). Similarly, it was found via wound healing and transwell analyses that MIR22HG upregulation could lead to a weakened migratory ability of SNU899 and SNU46 cells (Fig. 1F and G). All in all, MIR22HG expression is significantly downregulated and MIR22HG upregulation exerts restraining effects on cell proliferation and migration in laryngocarcinoma.

MIR22HG directly interacts with miR-5000-3p in laryngocarcinoma. To achieve the purpose of exploring the possible mechanism of MIR22HG in laryngocarcinoma, we determined the subcellular localization of MIR22HG in laryngocarcinoma cells with the application of subcellular fractionation and fluorescent *in situ* hybridization (FISH) assays. The result showed that MIR22HG was primarily distributed in the cytoplasm of SNU899 and SNU46 cells (Fig. 2A). We inferred from this that MIR22HG posttranscriptionally regulated gene expression and might act as a sponge of miRNA. After utilizing starBase (http://starbase.sysu.edu.cn/), miRNAs predicted to bind with MIR22HG under the screening condition (CLIP data: strict stringency, $\geq$5) were determined (Fig. 2B). An RNA pulldown assay was applied and showed that only miR-5000-3p was significantly enriched in the group of MIR22HG biotin probe, whereas no changes could be seen in other miRNAs (Fig. 2C). Figure 2D displays a binding site between MIR22HG and miR-5000-3p obtained from starBase. Subsequently, based on the results of a luciferase reporter assay, we discovered that overexpression of miR-5000-3p cut down the luciferase activity of pmirGLO-MIR22HG-WT but had no obvious effects on the luciferase activity of pmirGLO-MIR22HG-Mut (Fig. 2E). We then observed that miR-5000-3p upregulation had no effects on the expression of MIR22HG (Fig. 2F). Moreover, data from reverse transcription-quantitative PCR (RT-qPCR) analysis revealed a remarkable upregulation of miR-5000-3p expression in laryngocarcinoma cell lines (Fig. 2G). In addition, overexpressing MIR22HG in SNU46 and SNU899 cells could decrease the expression of miR-5000-3p (Fig. 2H). In addition, we adopted RT-qPCR to detect the efficacy of miR-5000-3p inhibition before conducting loss-of-function assays to analyze its function on laryngocarcinoma progression. As shown in Fig. 2I, the

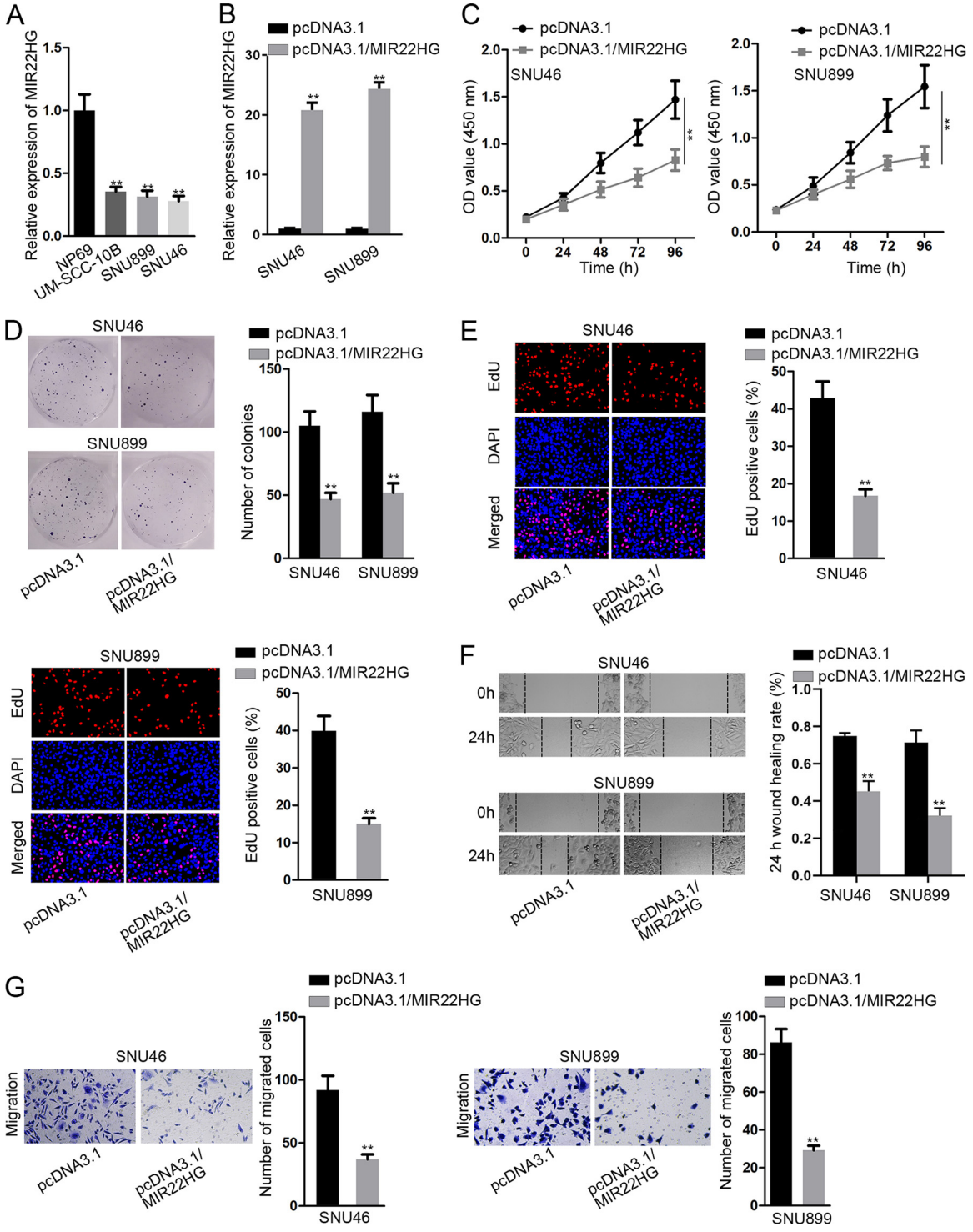

FIG 1 MIR22HG was expressed at low levels, and its upregulation inhibits cell proliferation and migration in laryngocarcinoma. (A) RT-qPCR analysis of MIR22HG expression in laryngocarcinoma cell lines (UM-SCC-10B, SNU899, and SNU46) and a normal nasopharyngeal epithelial cell line (NP69). (B) Measurement of the efficacy of MIR22HG overexpression in SNU46 and SNU899 cells by RT-qPCR. (C to E) Evaluation of cell proliferation ability in SNU46 and SNU899 cells transfected with pcDNA3.1/MIR22HG or pcDNA3.1 using CCK-8, colony formation, and EdU. (F and G) Evaluation of cell migratory ability in transfected cells by conducting wound healing and transwell assays. **, $P < 0.01$.

expression of miR-5000-3p was conspicuously reduced in SNU46 and SNU899 cells transfected with a miR-5000-3p inhibitor. The following cell proliferation assays revealed that miR-5000-3p suppression repressed the proliferation of SNU899 and SNU46 cells (Fig. 2J and K). Cell migration assays validated that the attenuated capability of cell

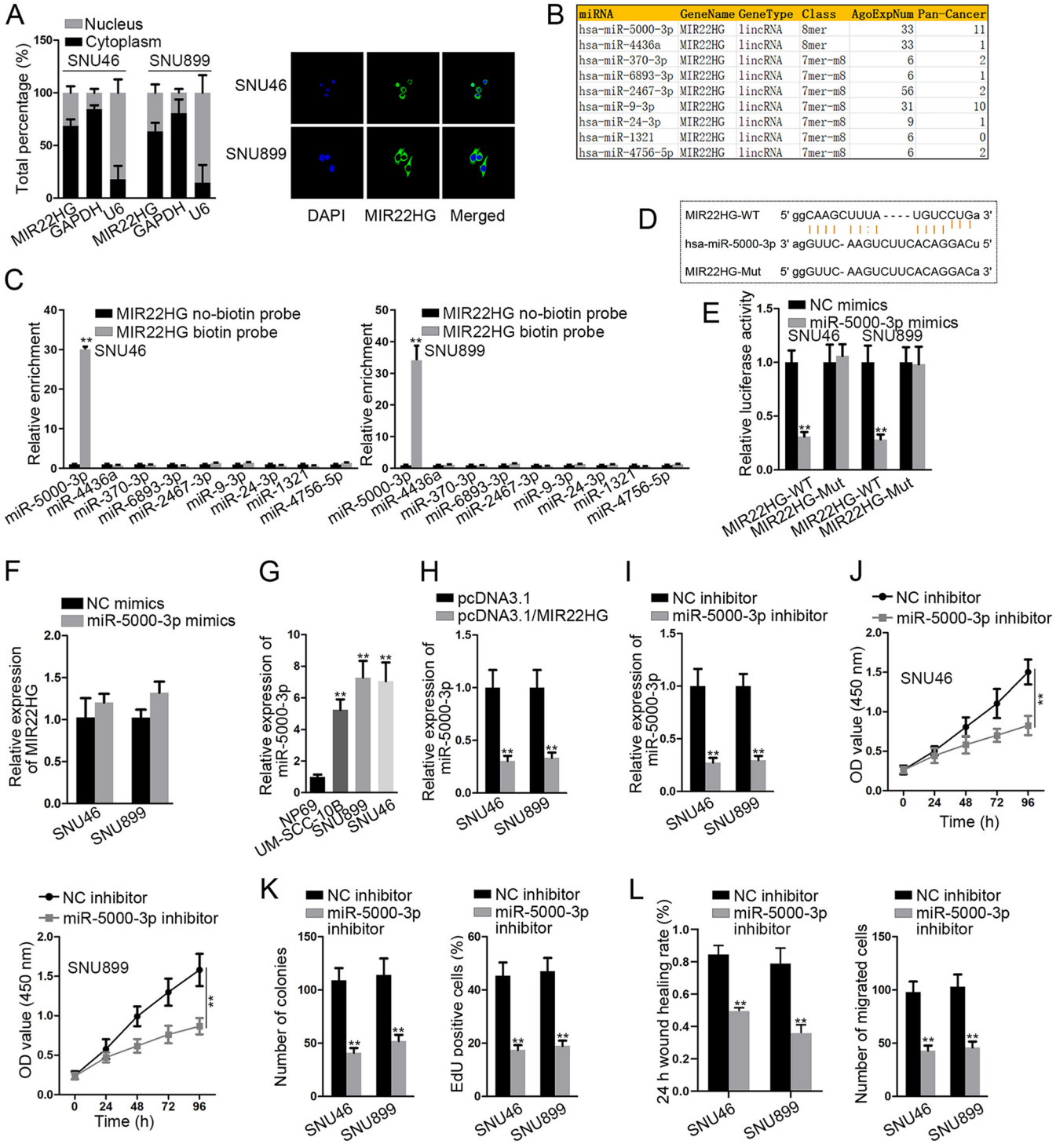

miRNA	GeneName	GeneType	Class	AgoExpNum	Pan-Cancer
hsa-miR-5000-3p	MIR22HG	lincRNA	8mer	33	11
hsa-miR-4436a	MIR22HG	lincRNA	8mer	33	1
hsa-miR-370-3p	MIR22HG	lincRNA	7mer-m8	6	2
hsa-miR-6893-3p	MIR22HG	lincRNA	7mer-m8	6	1
hsa-miR-2467-3p	MIR22HG	lincRNA	7mer-m8	56	2
hsa-miR-9-3p	MIR22HG	lincRNA	7mer-m8	31	10
hsa-miR-24-3p	MIR22HG	lincRNA	7mer-m8	9	1
hsa-miR-1321	MIR22HG	lincRNA	7mer-m8	6	0
hsa-miR-4756-5p	MIR22HG	lincRNA	7mer-m8	6	2

FIG 2 MIR22HG directly interacted with miR-5000-3p in laryngocarcinoma. (A) Detection the subcellular localization of MIR22HG in laryngocarcinoma cells with the application of subcellular fractionation and FISH assays. (B) miRNAs predicted to bind with MIR22HG based on the starBase database. (C) The binding capacity of MIR22HG and predicted miRNAs was analyzed via an RNA pulldown assay in SNU46 and SNU899 cells. (D) Binding site between MIR22HG and miR-5000-3p. (E) The interaction between MIR22HG and miR-5000-3p was confirmed by a luciferase reporter assay. (F) The effects of miR-5000-3p overexpression on MIR22HG were analyzed using qRT-PCR. (G) RT-qPCR analysis of miR-5000-3p expression in laryngocarcinoma cells and NP69 cells. (H) Analysis of miR-5000-3p expression in transfected cells via RT-qPCR. (I) RT-qPCR analysis of the efficacy of miR-5000-3p inhibition in SNU46 and SNU899 cells. (J and K) Evaluation of cell proliferative ability in SNU46 and SNU899 cells transfected with different plasmids utilizing CCK-8, colony formation, and EdU. (L) Analysis of cell migratory capability in different groups by applying wound healing and transwell assays. **, $P < 0.01$.

migration was induced by inhibition of miR-5000-3p in SNU46 and SNU899 cells (Fig. 2L). In brief, MIR22HG could bind to miR-5000-3p, and miR-5000-3p serves as an oncogene in laryngocarcinoma.

FBXW7 is a downstream target of miR-5000-3p in laryngocarcinoma. With the aim of finding the specific target gene of miR-5000-3p in laryngocarcinoma, we used starBase to predict the potential mRNAs that have the capacity of binding with miR-5000-3p under the screening condition (CLIP data: strict stringency, $\geq$5; degradome data: high stringency, $\geq$2). A Venn diagram demonstrating the overlaps of the microT, miRmap, and two mRNAs (FBXW7 and MTPN) is presented in Fig. 3A. Through RT-qPCR analysis, we observed that a significant increase in FBXW7 expression after miR-5000-3p expression was inhibited in SNU46 and SNU899 cells (Fig. 3B). Thus, FBXW7 was selected for further analysis. Compared to those in NP69 cells, FBXW7 expression and protein levels were markedly downregulated in laryngocarcinoma cells (Fig. 3C). Next, RT-qPCR and Western blot analyses suggested that upregulating MIR22HG expression in SNU46 and SNU899 cells resulted in a rise in the expression and protein levels of FBXW7 (Fig. 3D). Meanwhile, the expression and protein levels of FBXW7 were increased due to the downregulation of miR-5000-3p but diminished by the upregulation of miR-5000-3p (Fig. 3E). Later, a radioimmunoprecipitation assay (RIPA) revealed that MIR22HG, miR-5000-3p, and FBXW7 were observably enriched in the anti-Ago2 group, hinting that these RNAs exist in RNA-induced silencing complex (RISC) (Fig. 3F). Thereafter, a binding site between miR-5000-3p and FBXW7 was predicted using starBase (Fig. 3G). A luciferase reporter assay showed that miR-5000-3p upregulation could induce lower pmirGLO-FBXW7-WT luciferase activity but elicited no clear impact on pmirGLO-FBXW7-Mut luciferase activity (Fig. 3H). More importantly, MIR22HG upregulation elevated the expression and protein levels of FBXW7, but overexpression of miR-5000-3p could reverse the effect (Fig. 3I). To conclude, MIR22HG regulates FBXW7 expression by competitively binding with miR-5000-3p in laryngocarcinoma cells.

MIR22HG restrains laryngocarcinoma progression via the miR-5000-3p/FBXW7 axis. Based on these findings, we sought to test whether this ceRNA mechanism contributes to the initiation and development of laryngocarcinoma. SNU46 cell was transfected with sh-MIR22HG#1/2 to obtain low expression of MIR22HG (Fig. 4A). The rescue assays were conducted in cells transfected with negative control (NC) short hairpin RNA (sh-NC), sh-MIR22HG#1, and miR-5000-3p inhibitor. The data revealed that enhanced cell proliferation imposed by downregulation of MIR22HG was counteracted by miR-5000-3p depletion (Fig. 4B to D). In addition, the augmented migratory capacity made by MIR22HG silence was restored by miR-5000-3p downregulation (Fig. 4E and F). In contrast, the ectopic expression of miR-5000-3p offset the inhibitory effects of MIR22HG overexpression on cell proliferation and migration (Fig. 5). Furthermore, RT-qPCR analysis obtained a favorable efficacy of FBXW7 knockdown in SNU46 cells (Fig. 6A). Subsequently, cell proliferation assays showed that FBXW7 knockdown could countervail the suppressive effect of MIR22HG upregulation on cell proliferation (Fig. 6B to D). Moreover, wound healing and transwell assays showed that the repressive effect on cell migration induced by overexpressing MIR22HG could be reversed by FBXW7 depletion (Fig. 6E and F). We assumed that the mutated MIR22HG could affect the course of laryngocarcinoma by regulating miR-5000-3p. At the beginning, the RT-qPCR data showed that mutant MIR22HG had no impact on the expression of miR-5000-3p (Fig. 6G). The subsequent functional assays showed that mutant MIR22HG upregulation could not disturb cell proliferation and migration in laryngocarcinoma (Fig. 6H). We also investigated whether miR-5000-3p modulated the growth of laryngocarcinoma by modulating mutant FBXW7. We observed no changes for mutant FBXW7 in mRNA and protein expression in cells transfected with miR-5000-3p mimics using RT-qPCR and Western blot analyses (Fig. 6I). The rescue assays demonstrated that the effects of miR-5000-3p upregulation on proliferation and migration could not be restored by

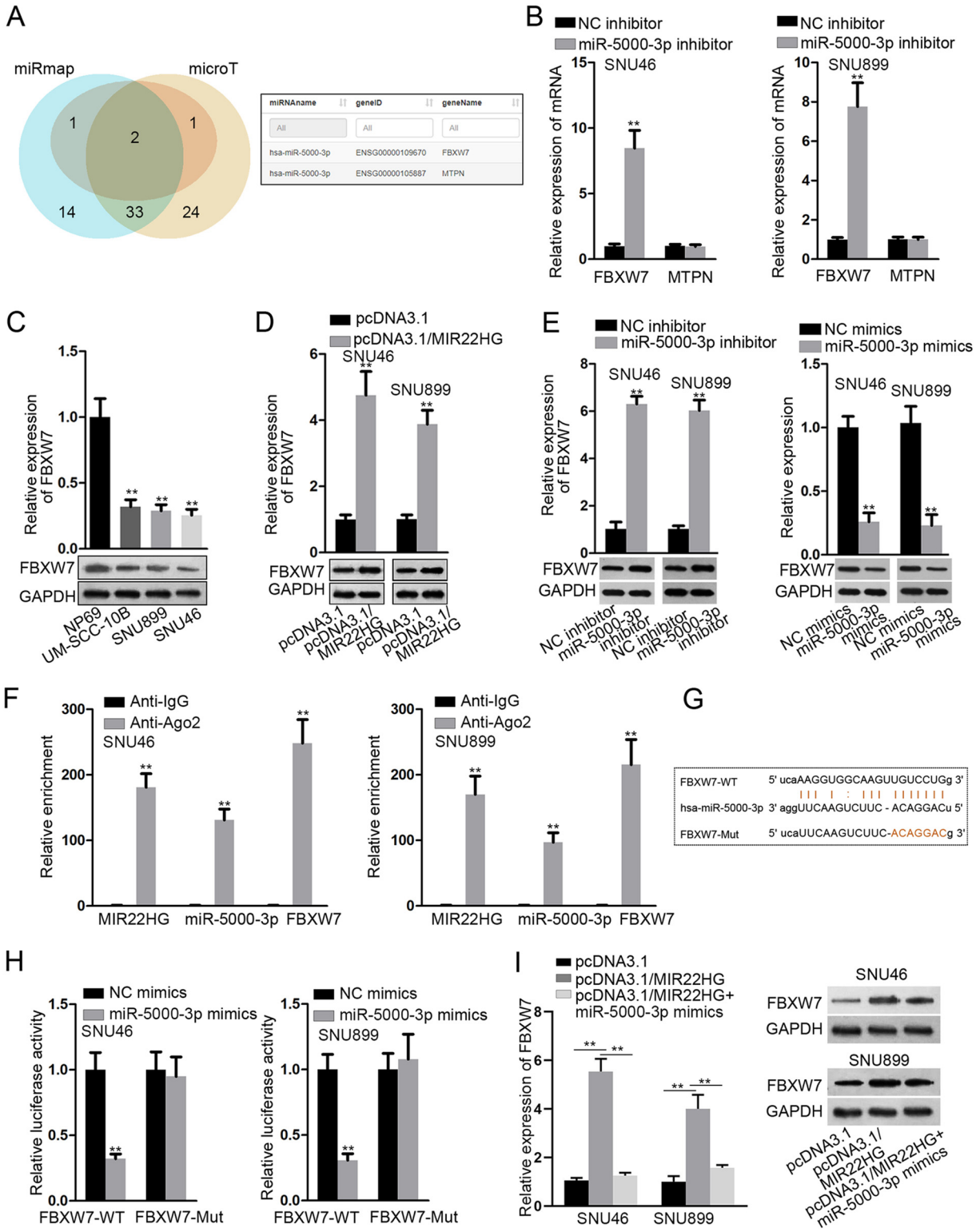

FIG 3 FBXW7 was the downstream target of miR-5000-3p in laryngocarcinoma. (A) Analysis overlaps illustrated by a Venn diagram. (B) RT-qPCR analysis of FBXW7 expression in SNU46 and SNU899 cells transfected with miR-5000-3p inhibitor or NC inhibitor. (C) RT-qPCR and Western blot analyses of FBXW7 expression in laryngocarcinoma cells and NP69 cells. (D) Measurement of FBXW7 expression in transfected cells through RT-qPCR and Western blotting. (E) FBXW7 expression and protein levels were appraised by RT-qPCR and Western blotting in cells with miR-5000-3p inhibitor or mimics. (F) The existence of RNAs (MIR22HG, miR-5000-3p and FBXW7) in RISC confirmed by RIPA. (G) Binding site between miR-5000-3p and FBXW7 predicted using starBase. (H) Interaction between miR-5000-3p and FBXW7 validated using a luciferase reporter assay. (I) Measurement of FBXW7 expression in different groups via RT-qPCR and Western blotting. **, $P < 0.01$.

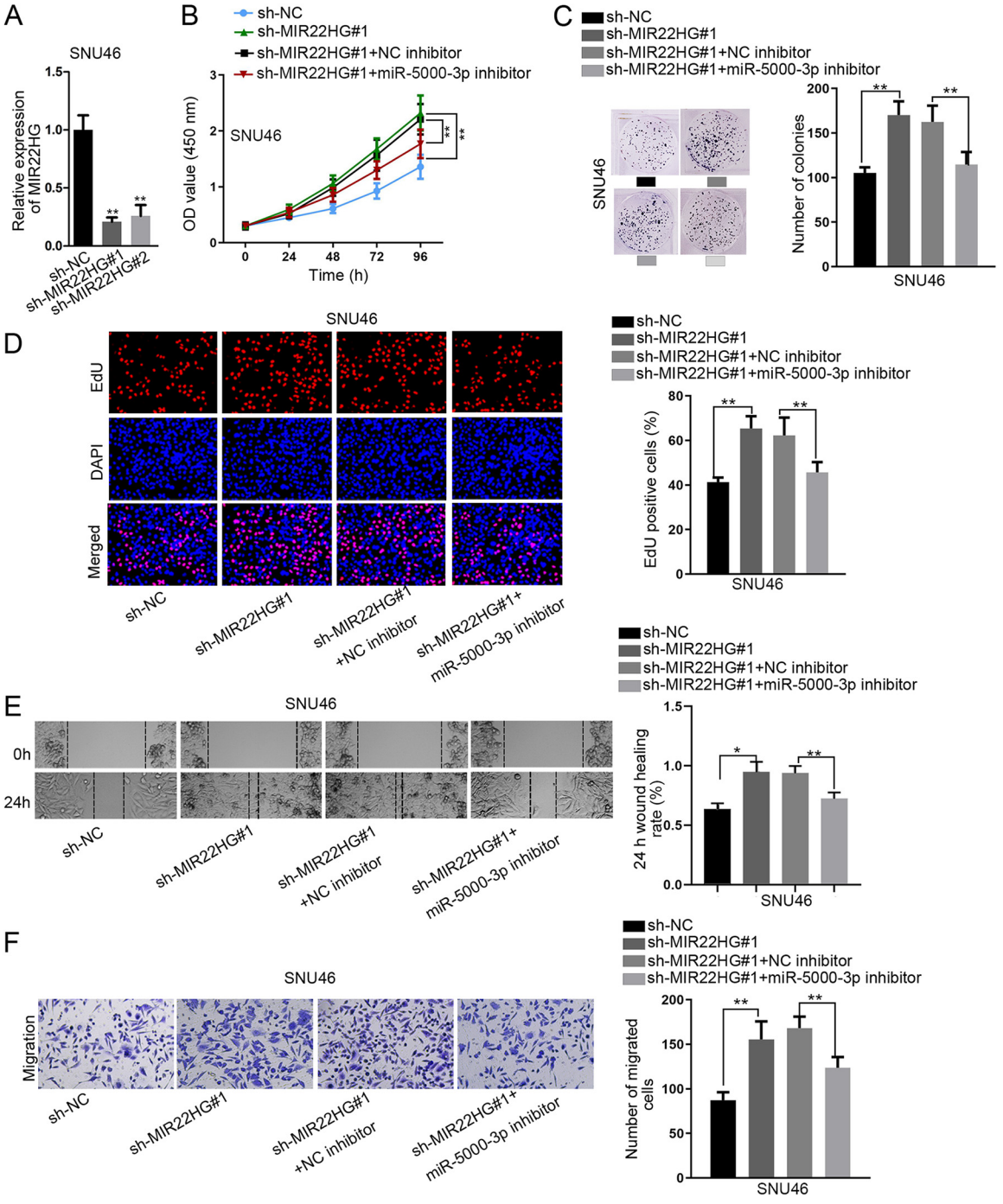

FIG 4 miR-5000-3p inhibition recovered the impacts of MIR22HG silence on cell proliferation and migration. (A) The downregulation of MIR22HG in SNU46 cells was confirmed by qRT-PCR. (B to D) Cell proliferative abilities were examined by using CCK-8, colony formation, and EdU assays. (E and F) The migratory abilities were evaluated in wound healing and transwell assays. **, $P < 0.01$.

mutant FBXW7 overexpression (Fig. 6J). All of these data show that the MIR22HG/miR-5000-3p/FBXW7 pathway contributes to the progression of laryngocarcinoma.

E2F6 inhibits MIR22HG transcription in laryngocarcinoma. After exploration on the downstream mechanism of MIR22HG, we investigated the upstream mechanism of MIR22HG in laryngocarcinoma. By using the UCSC database (http://genome.ucsc.edu/), E2F6 was predicted as a transcription repressor of MIR22HG. To verify this prediction, we first overexpressed E2F6 in SNU46 and SNU899 cells (Fig. 7A) and then discovered that the expression of MIR22HG was remarkably reduced by E2F6 overexpression

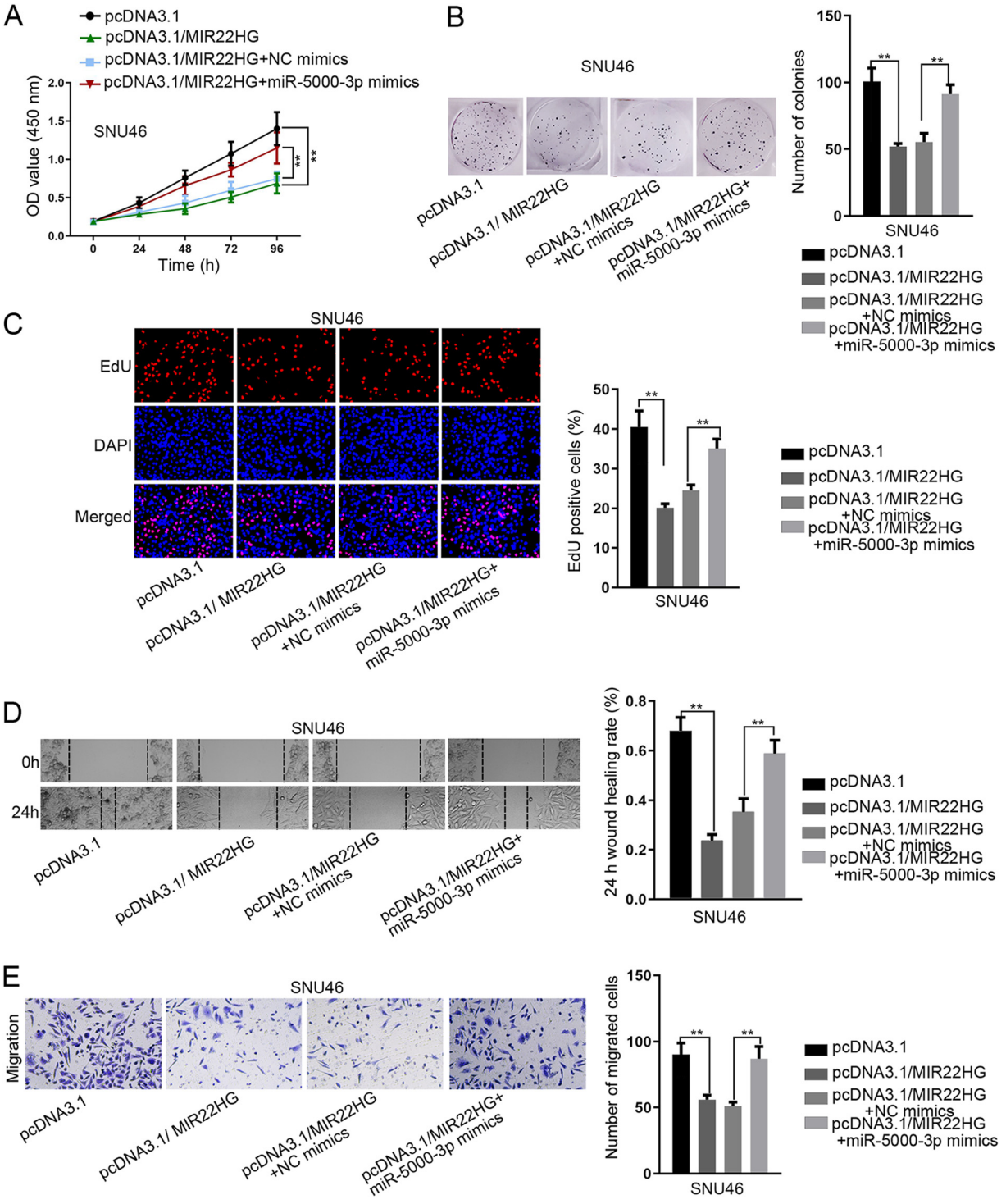

FIG 5 The suppressed function of MIR22HG-overexpressed SNU46 cells was normalized by enhanced miR-5000-3p. (A to C) Evaluation of cell proliferation ability in SNU46 cells transfected with different plasmids by conducting cell proliferation assays. (D and E) Analysis of cell migration capability in different groups by carrying out cell migration assays. **, $P < 0.01$.

(Fig. 7B). In addition, the DNA motif of E2F6 was obtained through utilizing JASPAR (http://jaspar.genereg.net/) (Fig. 7C). Furthermore, there were two binding sites between E2F6 and the MIR22HG promoter (Fig. 7D). Moreover, a chromatin immunoprecipitation (ChIP) assay verified the binding capacity of E2F6 and the MIR22HG promoter in SNU46 and SNU899 cells (Fig. 7E). In addition, a luciferase reporter assay validated

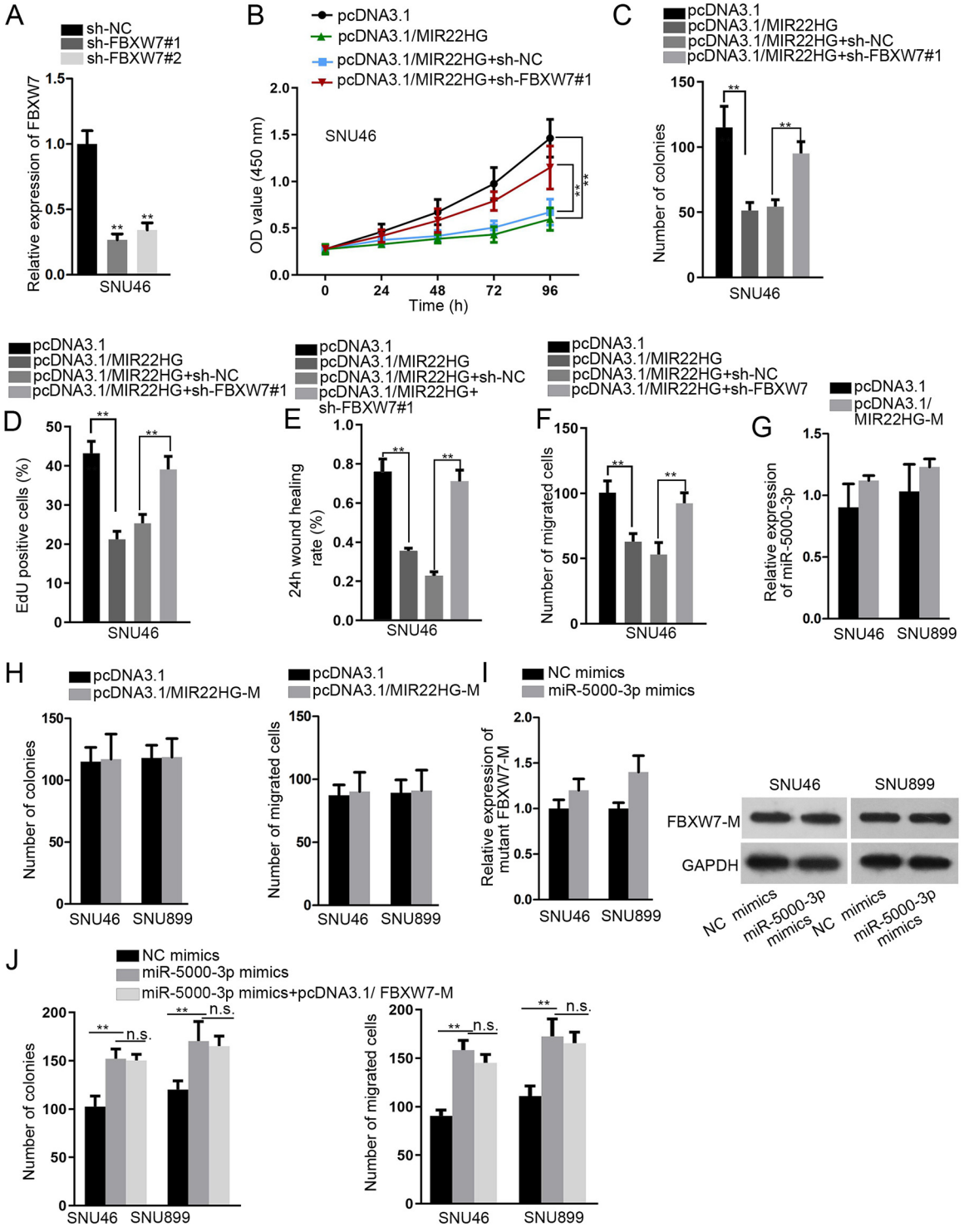

FIG 6 MIR22HG affected laryngocarcinoma cell proliferation and migration by targeting FBXW7. (A) Measurement of the efficacy of FBXW7 knockdown in SNU46 cells via RT-qPCR. (B to D) Cell proliferation was assessed in rescue assays. (E and F) Cell migration was examined in rescue assays. (G) RT-qPCR detected the expression of miR-5000-3p in cells transfected with mutant MIR22HG (MIR22HG-M). (H) The effects of MIR22HG-M on proliferation and migration were analyzed by using colony formation and transwell assays. (I) RT-qPCR and Western blot analyses of mRNA and protein expression of mutant FBXW7 (FBXW7-M). (J) Colony formation and transwell assays revealed that FBXW7-M had no impact on miR-5000-3p-regulated proliferation and migration.**, $P < 0.01$; n.s., not significant.

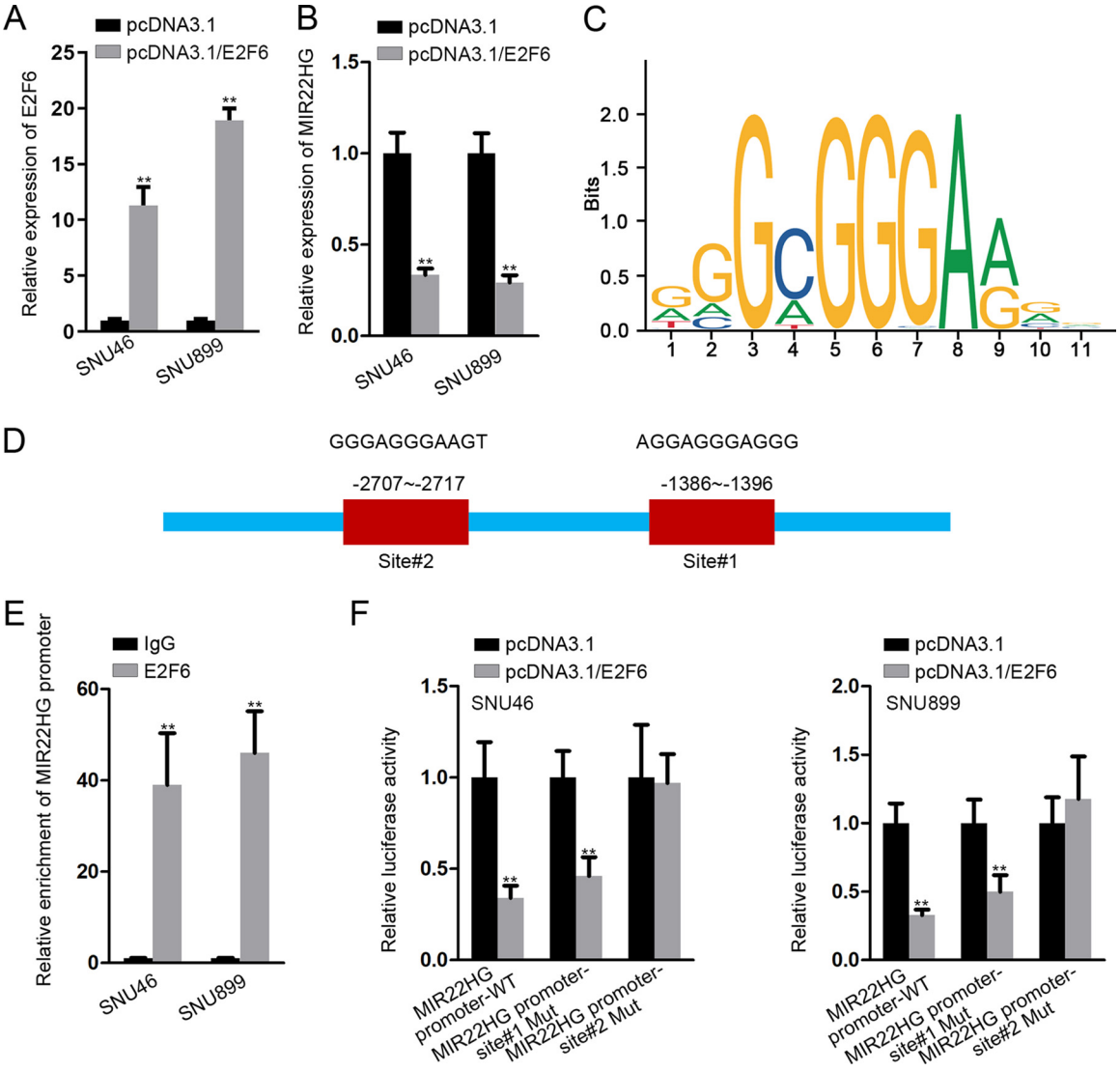

FIG 7 E2F6 inhibited MIR22HG transcription in laryngocarcinoma. (A) RT-qPCR analysis of the efficacy of E2F6 overexpression in SNU46 and SNU899 cells. (B) RT-qPCR analysis of the expression of MIR22HG in transfected cells. (C) DNA motif of E2F6 obtained from JASPAR. (D) Two binding sites between E2F6 and MIR22HG promoter in SNU46 and SNU899 cells. (E and F) Binding sites between E2F6 and MIR22HG promoter analyzed by ChIP and luciferase reporter assays. **, $P < 0.01$.

that E2F6 bound to the MIR22HG promoter at site 2 (Fig. 7F). In sum, E2F6 restrains MIR22HG transcription in laryngocarcinoma.

DISCUSSION

Increasing studies have revealed the significant function of lncRNAs on the complicated courses involved in the biological progression of laryngocarcinoma. For example, lncRNA NEAT1 plays oncogenic roles in laryngocarcinoma by sponging miR-29a-3p (24). Elevated expression of lncRNA TUG1 facilitates laryngocarcinoma development via the miR-145-5p/ROCK1 axis (25). lncRNA PCAT19 accelerates laryngocarcinoma cell proliferation through the miR-182/PDK4 pathway (26). Recent researches have revealed the antitumor role of MIR22HG in several cancers, such as gastric cancer and endometrial carcinoma (22, 23). However, the underlying role of MIR22HG in laryngocarcinoma remains to be detected. In this study, MIR22HG was expressed at significantly low levels, and MIR22HG upregulation exerted repressive effects on both cell proliferation and migration in laryngocarcinoma cells.

Plenty of evidence suggested that lncRNAs may exert crucial effects on the tumorigen-

esis and development of human cancers via sponging particular miRNA (24, 27). miR-5000-3p, a previously researched miRNA, has been suggested to be a potential biomarker in colon cancer (28). In the present study we found that, according to bioinformatics prediction and mechanism assays, miR-5000-3p bound with MIR22HG in laryngocarcinoma cells. Recently, a target-directed miRNA degradation mechanism analysis suggested that miRNA was decayed by targeting mRNA (29). Based on this theory, we assumed that miR-5000-3p would be decayed by some specific mRNAs. Since this mechanism was so complicated, with numerous explanations, we will study this mechanism in the future to examine the possible mRNAs that could degrade miR-5000-3p. In addition, MIR22HG negatively regulated the expression of miR-5000-3p in laryngocarcinoma. Moreover, miR-5000-3p was verified to promote laryngocarcinoma cell proliferation and migration. Rescue assays showed that downregulation of miR-5000-3p could reverse the influence imposed by MIR22HG silence on laryngocarcinoma progression and that the overexpression of miR-5000-3p could offset the effects made by the upregulation of MIR22HG.

FBXW7 (F-box and WD repeat domain containing 7) has been confirmed to function as a tumor suppressor in multiple investigations related to human malignancies. For instance, FBXW7 restrains the epithelial-to-mesenchymal transition (EMT) process in non-small-cell lung cancer (30). FBXW7 inhibits cholangiocarcinoma progression via NOTCH1 and MCL1 (31). In the present study, the FBXW7 gene was shown to be a downstream target gene of miR-5000-3p in laryngocarcinoma. In addition, rescue assays revealed that the repressive effects on laryngocarcinoma cell proliferation and migration resulting from overexpressing MIR22HG could be recovered by FBXW7 depletion or miR-5000-3p upregulation. More interestingly, the overexpression of mutant FBXW7 could counteract the influence of miR-5000-3p upregulation as well, and the effect was more conspicuous than that of normal FBXW7 overexpression.

The E2F transcription factor 6 (E2F6) gene has been verified to be an oncogene and transcriptional repressor in ovarian cancer (32). In addition, the expression of LINC01436 in non-small-cell lung cancer is transcriptionally suppressed by E2F6 under normoxia (33). Moreover, E2F6-induced downregulation of lncRNA CASC2 contributes to gastric cancer progression (34). In this research, E2F6 was proved to be capable of inhibiting MIR22HG transcription in laryngocarcinoma.

In conclusion, E2F6-mediated downregulation of MIR22HG facilitates laryngocarcinoma progression via the miR-5000-3p/FBXW7 axis. This finding suggests that MIR22HG may be utilized as a promising biomarker for laryngocarcinoma treatment. Future studies will further enrich and explore the molecular mechanism of MIR22HG upstream and downstream, as well as whether there are other miRNAs and mRNAs involved, which will also be the focus of our next study.

MATERIALS AND METHODS

Cell culture. A normal human nasopharyngeal epithelial cell line (NP69) and laryngocarcinoma cell lines (UM-SCC-10B, SNU899, and SNU46) were purchased from the American Type Culture Collection (ATCC) and Invitrogen (Carlsbad, CA). The cells were cultured in Dulbecco modified Eagle medium (Invitrogen) that was supplied with 10% fetal bovine serum (FBS; Invitrogen) and 1% penicillin-streptomycin (Sigma-Aldrich, Milan, Italy) at 37°C in a 5% CO_2 incubator.

Cell transfection. SNU46 and SNU899 cells were transfected with short hairpin RNAs (shRNAs) against FBXW7 (sh-FBXW7#1#2) and their corresponding NC (sh-NC), pcDNA3.1/MIR22HG, pcDNA3.1/E2F6, and empty pcDNA3.1 vectors, separately. The miR-5000-3p mimics, miR-5000-3p inhibitor, NC mimics, and NC inhibitor were synthesized by GenePharma (Shanghai, China). The cell transfections after 48 h were routinely conducted using Lipofectamine 2000 (Invitrogen).

RT-qPCR. Total RNA was separated with usage of TRIzol reagent (Invitrogen). Briefly, cDNA was synthesized by using a Maxima first-strand cDNA synthesis kit (Promega, Madison, WI). RT-qPCR was carried out with a SYBR Premix Ex Taq kit (TaKaRa, Tokyo, Japan) on an ABI 7500 RT-PCR system (Applied Biosystems, Foster City, CA). The $2^{-\Delta\Delta CT}$ method was applied to calculate the relative expression levels. GAPDH/U6 was used as the normalization control.

CCK-8 assay. In brief, 1×10^3 SNU46 and SNU899 cells were first inoculated in 96-well plates and cultivated over specific time points. Then, 10 μl of the CCK-8 reagent was added, followed by incubation for an additional 4 h. A microplate reader (Bio-Tek Instruments, Hopkinton, MA) at an absorbance of 450 nm was used to evaluate cell viability.

Colony formation assay. After transfection, 1×10^3 cells were seeded into six-well plates for cultivation. The medium was replaced when needed, usually every 3 days. The colonies were then fixed

in methanol (Sigma-Aldrich) and stained with crystal violet (Sigma-Aldrich). Visible colonies (≥50 cells) were then counted manually.

Wound healing assay. Cell migration was assessed by using a wound-healing assay. Briefly, at 48 h after transfection, the cells were added to six-well plates. When the cells reached 80% confluence, the cell monolayer was scratched using a sterile plastic micropipette tip, and the cells were then incubated under standard conditions. After 24 h, images of the wound were obtained and analyzed under an inverted microscope (Olympus, Tokyo, Japan).

Western blotting. We obtained proteins from cells which were lysed using RIPA lysis buffer containing protease inhibitors. Protein concentrations were quantified using a BCA protein assay (Invitrogen). Proteins were separated by SDS-PAGE (Bio-Rad, Hercules, CA) and moved to polyvinylidene difluoride membranes (Millipore, Billerica, MA). After being sealed with 5% nonfat milk, the membranes were cultivated with primary antibodies to FBXW7 (ab227677), TPM1 (ab55915), and GAPDH (ab8245) from Abcam (Cambridge). Secondary antibodies were added for cultivation for 1 h. GAPDH was used as an internal control. The amount of protein was determined using a chemiluminescence detection system.

Migration assay. Migration capacities were assessed by using Transwell chambers. A total of 2×10^4 cells in the top compartment was added with serum-free medium, while culture medium with an additional 10% FBS was placed in the lower chamber. The lower surfaces of the membranes were fixed using methanol and stained with crystal violet to count the cells. The number of migratory cells was observed under an optical microscope (Olympus).

Subcellular fractionation. To explore cellular localization of MIR22HG, cytosolic and nuclear fractions were collected by using a nuclear/cytoplasmic isolation kit (Biovision, Milpitas, CA). RNAs were obtained from each fraction and subjected to RT-qPCR to evaluate the levels of MIR22HG, U6 (nuclear control), and GAPDH (cytoplasmic control).

FISH assay. SNU46 and SNU899 cells were fixed in 4% formaldehyde and then cleaned with phosphate-buffered saline. After dehydration with ethanol, the dried cells were blended with a FISH probe (Ribobio, Guangzhou, China) in hybridization buffer and cultivated for 2 min. The slides were then rinsed, dehydrated, and visualized with DAPI (4′,6′diamidino-2-phenylindole). The cells were observed using a fluorescence microscope (Olympus).

EdU incorporation assay. Transfected cells were plated in 96-well plate, and the culture medium was changed to a medium containing 20 mM EdU. After incubation for 2 h, the cells were dyed with DAPI, and the dye images were obtained using an inverted fluorescence microscope (Olympus).

RNA pulldown assay. In brief, MIR22HG biotin and MIR22HG nonbiotin probes constructed by GenePharma were treated with M-280 streptavidin-magnetic beads (Invitrogen) to produce probe-coated beads. The cells were then gathered and lysed, followed by sonication and incubating with probe-coated beads overnight. RNA complexes bound to the beads after purification were detected using RT-qPCR analysis.

Luciferase reporter assay. The wild-type (WT) and mutant (Mut) binding sites of miR-5000-3p in the MIR22HG sequence or the FBXW7 3′ untranslated region were subcloned into pmirGLO Dual-Luciferase vector to generate MIR22HG-WT/Mut or FBXW7-WT/Mut and then cotransfected with miR-5000-3p mimics or NC mimics into SNU46 and SNU899 cells. The pGL3-MIR22HG promoter was cotransfected with pcDNA3.1/E2F6 or pcDNA3.1 vector into cells. The luciferase activity was examined by using a Dual-Luciferase reporter assay system (Promega).

RIPA. We conducted the RIPA experiments by using a Magna RNA immunoprecipitation kit (Millipore). SNU46 and SNU899 cells were lysed in RIPA lysis buffer, and cell extracts were then cultivated with magnetic beads conjugated with anti-IgG or anti-Ago2 (Millipore). In order to remove the protein, the beads were incubated with proteinase K after rinsing. Finally, the relative enrichment of miR-5000-3p, MIR22HG, and FBXW7 was analyzed by real-time PCR.

ChIP assay. A ChIP experiment was performed with SNU46 and SNU899 cells using a Magna ChIP A/G kit (Millipore). In brief, cells fixed with formaldehyde were first gathered and subjected to lysis buffer. Later, the lysate was sonicated to 200- to 300-bp fragments, followed by incubation with anti-E2F6 or anti-IgG. Next, ChIP-enriched DNA samples were quantified using RT-qPCR to determine the E2F6 binding sites of MIR22HG promoter region.

Statistical analysis. We performed statistical analysis using Prism 5 software (GraphPad, La Jolla, CA). Experimental data are expressed as means ± standard deviations. Differences between two or more groups were estimated using a Student *t* test or one-way analysis of variance (ANOVA). A *P* value of <0.05 was considered statistically significant. At least three independent experiments were performed for each analysis.

ACKNOWLEDGMENTS

We thank all participants in this study.

There were no conflicts of interest.

REFERENCES

1. McGuire S. 2016. World cancer report 2014—Geneva, Switzerland: World Health Organization, International Agency for Research on Cancer, WHO Press, 2015. Adv Nutr 7:418–419.
2. Miller KD, Goding Sauer A, Ortiz AP, Fedewa SA, Pinheiro PS, Tortolero-Luna G, Martinez-Tyson D, Jemal A, Siegel RL. 2018. Cancer statistics for Hispanics/Latinos, 2018. CA Cancer J Clin 68:425–445. https://doi.org/10.3322/caac.21494.
3. Lampri ES, Chondrogiannis G, Ioachim E, Varouktsi A, Mitselou A, Galani A, Briassoulis E, Kanavaros P, Galani V. 2015. Biomarkers of head and neck cancer, tools or a gordian knot? Int J Clin Exp Med 8:10340–10357.

4. Li P, Liu H, Wang Z, He F, Wang H, Shi Z, Yang A, Ye J. 2016. MicroRNAs in laryngeal cancer: implications for diagnosis, prognosis and therapy. Am J Transl Res 8:1935–1944.
5. Hoffman HT, Porter K, Karnell LH, Cooper JS, Weber RS, Langer CJ, Ang KK, Gay G, Stewart A, Robinson RA. 2006. Laryngeal cancer in the United States: changes in demographics, patterns of care, and survival. Laryngoscope 116:1–13. https://doi.org/10.1097/01.mlg.0000236095.97947.26.
6. Marioni G, Marchese-Ragona R, Cartei G, Marchese F, Staffieri A. 2006. Current opinion in diagnosis and treatment of laryngeal carcinoma. Cancer Treat Rev 32:504–515. https://doi.org/10.1016/j.ctrv.2006.07.002.
7. Larbcharoensub N, Cheewaruangroj W, Nitiyanant P. 2011. Laryngeal sarcocystosis accompanying laryngeal squamous cell carcinoma: case report and literature review. Southeast Asian J Trop Med Public Health 42:1072–1076.
8. Gama RR, Carvalho AL, Longatto Filho A, Scorsato AP, López RVM, Rautava J, Syrjänen S, Syrjänen K. 2016. Detection of human papillomavirus in laryngeal squamous cell carcinoma: systematic review and meta-analysis. Laryngoscope 126:885–893. https://doi.org/10.1002/lary.25738.
9. Markou K, Christoforidou A, Karasmanis I, Tsiropoulos G, Triaridis S, Constantinidis I, Vital V, Nikolaou A. 2013. Laryngeal cancer: epidemiological data from northern Greece and review of the literature. Hippokratia 17:313–318.
10. He FY, Liu HJ, Guo Q, Sheng JL. 2017. Reduced miR-300 expression predicts poor prognosis in patients with laryngeal squamous cell carcinoma. Eur Rev Med Pharmacol Sci 21:760–764.
11. Cao WJ, Wu HL, He BS, Zhang YS, Zhang ZY. 2013. Analysis of long noncoding RNA expression profiles in gastric cancer. World J Gastroenterol 19:3658–3664. https://doi.org/10.3748/wjg.v19.i23.3658.
12. Cheng Y, Liu X, Zhang S, Lin Y, Yang J, Zhang C. 2009. MicroRNA-21 protects against the H_2O_2-induced injury on cardiac myocytes via its target gene PDCD4. J Mol Cell Cardiol 47:5–14. https://doi.org/10.1016/j.yjmcc.2009.01.008.
13. Fagan-Solis KD, Schneider SS, Pentecost BT, Bentley BA, Otis CN, Gierthy JF, Arcaro KF. 2013. The RhoA pathway mediates MMP-2 and MMP-9-independent invasive behavior in a triple-negative breast cancer cell line. J Cell Biochem 114:1385–1394. https://doi.org/10.1002/jcb.24480.
14. Guo W, Ren D, Chen X, Tu X, Huang S, Wang M, Song L, Zou X, Peng X. 2013. HEF1 promotes epithelial mesenchymal transition and bone invasion in prostate cancer under the regulation of microRNA-145. J Cell Biochem 114:1606–1615. https://doi.org/10.1002/jcb.24502.
15. Ponting CP, Oliver PL, Reik W. 2009. Evolution and functions of long noncoding RNAs. Cell 136:629–641. https://doi.org/10.1016/j.cell.2009.02.006.
16. Xiang J, Guo S, Jiang S, Xu Y, Li J, Li L, Xiang J. 2016. Silencing of long non-coding RNA MALAT1 promotes apoptosis of glioma cells. J Korean Med Sci 31:688–694. https://doi.org/10.3346/jkms.2016.31.5.688.
17. Evans JR, Feng FY, Chinnaiyan AM. 2016. The bright side of dark matter: lncRNAs in cancer. J Clin Invest 126:2775–2782. https://doi.org/10.1172/JCI84421.
18. Gibb EA, Vucic EA, Enfield KS, Stewart GL, Lonergan KM, Kennett JY, Becker-Santos DD, MacAulay CE, Lam S, Brown CJ, Lam WL. 2011. Human cancer long noncoding RNA transcriptomes. PLoS One 6:e25915. https://doi.org/10.1371/journal.pone.0025915.
19. Moran VA, Perera RJ, Khalil AM. 2012. Emerging functional and mechanistic paradigms of mammalian long noncoding RNAs. Nucleic Acids Res 40:6391–6400. https://doi.org/10.1093/nar/gks296.
20. Long B, Li N, Xu XX, Li XX, Xu XJ, Liu JY, Wu ZH. 2018. Long noncoding RNA LOXL1-AS1 regulates prostate cancer cell proliferation and cell cycle progression through miR-541-3p and CCND1. Biochem Biophys Res Commun 505:561–568. https://doi.org/10.1016/j.bbrc.2018.09.160.
21. Wang YG, Wang T, Shi M, Zhai B. 2019. Long noncoding RNA EPB41L4A-AS2 inhibits hepatocellular carcinoma development by sponging miR-301a-5p and targeting FOXL1. J Exp Clin Cancer Res 38:153. https://doi.org/10.1186/s13046-019-1128-9.
22. Li H, Wang Y. 2019. Long noncoding RNA (lncRNA) MIR22HG suppresses gastric cancer progression through attenuating NOTCH2 signaling. Med Sci Monit 25:656–665. https://doi.org/10.12659/MSM.912813.
23. Cui Z, An X, Li J, Liu Q, Liu W. 2018. LncRNA MIR22HG negatively regulates miR-141-3p to enhance DAPK1 expression and inhibits endometrial carcinoma cells proliferation. Biomed Pharmacother 104:223–228. https://doi.org/10.1016/j.biopha.2018.05.046.
24. Liu T, Wang W, Xu YC, Li ZW, Zhou J. 2019. Long noncoding RNA NEAT1 functions as an oncogene in human laryngocarcinoma by targeting miR-29a-3p. Eur Rev Med Pharmacol Sci 23:6234–6241. https://doi.org/10.26355/eurrev_201907_18442.
25. Zhuang S, Liu F, Wu P. 2019. Upregulation of long noncoding RNA TUG1 contributes to the development of laryngocarcinoma by targeting miR-145-5p/ROCK1 axis. J Cell Biochem 120:13392–13402. https://doi.org/10.1002/jcb.28614.
26. Xu S, Guo J, Zhang W. 2019. lncRNA PCAT19 promotes the proliferation of laryngocarcinoma cells via modulation of the miR-182/PDK4 axis. J Cell Biochem 120:12810–12821. https://doi.org/10.1002/jcb.28552.
27. Jiang C, Yang Y, Yang Y, Guo L, Huang J, Liu X, Wu C, Zou J. 2018. Long noncoding RNA (lncRNA) HOTAIR affects tumorigenesis and metastasis of non-small cell lung cancer by upregulating miR-613. Oncol Res 26:725–734. https://doi.org/10.3727/096504017X15119467381615.
28. Xia ZS, Wang L, Yu T, Zhong W, Lian GD, Wu D, Zhou HM, Chen GC. 2014. miR-5000-3p, miR-5009-3P and miR-552: potential microRNA biomarkers of side population cells in colon cancer. Oncol Rep 32:589–596. https://doi.org/10.3892/or.2014.3232.
29. Ghini F, Rubolino C, Climent M, Simeone I, Marzi MJ, Nicassio F. 2018. Endogenous transcripts control miRNA levels and activity in mammalian cells by target-directed miRNA degradation. Nat Commun 9:3119. https://doi.org/10.1038/s41467-018-05182-9.
30. Xiao G, Li Y, Wang M, Li X, Qin S, Sun X, Liang R, Zhang B, Du N, Xu C, Ren H, Liu D. 2018. FBXW7 suppresses epithelial-mesenchymal transition and chemo-resistance of non-small-cell lung cancer cells by targeting snai1 for ubiquitin-dependent degradation. Cell Prolif 51:e12473. https://doi.org/10.1111/cpr.12473.
31. Mori A, Masuda K, Ohtsuka H, Shijo M, Ariake K, Fukase K, Sakata N, Mizuma M, Morikawa T, Hayashi H, Nakagawa K, Motoi F, Naitoh T, Fujishima F, Unno M. 2018. FBXW7 modulates malignant potential and cisplatin-induced apoptosis in cholangiocarcinoma through NOTCH1 and MCL1. Cancer Sci 109:3883–3895. https://doi.org/10.1111/cas.13829.
32. Cheng FHC, Lin HY, Hwang TW, Chen YC, Huang RL, Chang CB, Yang W, Lin RI, Lin CW, Chen GCW, Mai SY, Lin JMJ, Chuang YM, Chou JL, Kuo LW, Li C, Cheng ASL, Lai HC, Wu SF, Tsai JC, Chan M. 2019. E2F6 functions as a competing endogenous RNA, and transcriptional repressor, to promote ovarian cancer stemness. Cancer Sci 110:1085–1095. https://doi.org/10.1111/cas.13920.
33. Yuan S, Xiang Y, Wang G, Zhou M, Meng G, Liu Q, Hu Z, Li C, Xie W, Wu N, Wu L, Cai T, Ma X, Zhang Y, Yu Z, Bai L, Li Y. 2019. Hypoxia-sensitive LINC01436 is regulated by E2F6 and acts as an oncogene by targeting miR-30a-3p in non-small cell lung cancer. Mol Oncol 13:840–856. https://doi.org/10.1002/1878-0261.12437.
34. Li Y, Jiang L, Lv S, Xu H, Fan Z, He Y, Wen H. 2019. E2F6-mediated lncRNA CASC2 down-regulation predicts poor prognosis and promotes progression in gastric carcinoma. Life Sci 232:116649. https://doi.org/10.1016/j.lfs.2019.116649.